Journal of Energy Storage 86 (2024) 111138

Contents lists available at ScienceDirect

Journal of Energy Storage

journal homepage: www.elsevier.com/locate/est

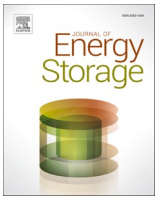

Research papers

How pressure affects costs of power conversion machinery in compressed air energy storage; part II: Heat exchangers

Zahra Baniamerian [a,*], Seamus Garvey [a], James Rouse [a], Bruno Cárdenas [a], Daniel L. Pottie [b], Edward R. Barbour [b], Audrius Bagdanavicius [c]

[a] Mechanical and Aerospace Systems Research Group, University of Nottingham, Nottingham NG7 2TU, UK
[b] Centre for Renewable Energy System Technology (CREST), Loughborough University, Loughborough LE11 3TU, UK
[c] School of Engineering, University of Leicester, Leicester LE1 7RH, UK

ARTICLE INFO

Keywords:
Compressed air energy storage
Operating pressure
Storage pressure
Heat exchanger
Cost per kW

ABSTRACT

In the field of compressed air energy storage, a critical economic aspect that has been overlooked in existing literature relates to the influence of storage pressure on the capital cost of power conversion system. In Part I, a comprehensive study was conducted to address this question focusing on compressors and expanders. This part is devoted to the heat exchangers and basically assesses the engineering rationale behind the relationship between the cost per kW for HXs and operating pressure. Based on the performed analysis, the operating pressure of a HX impacts two crucial cost-related factors: the heat transfer area and required tube thicknesses. Higher operating pressures are associated with the smaller heat transfer area tending to lower costs, but increasing pressure raises tube thickness requirements, tending to increase costs. Below approximately 200 bar, the former effect prevails over the latter, leading to cost reductions with rising pressure. Conversely, at higher pressures, the latter effect outweighs the former, resulting in cost increases with increasing pressure. On the other hand, as the number of compression stages is increased to attain higher storage pressures, there is a noteworthy variation in the cost contribution of HXs. Specifically, the contribution of HX costs within the PCS machinery escalates from 10 % at a storage pressure of 30 bar to approximately 35% at a storage pressure of 350bar. This cost increase is accompanied by a substantial reduction in costs associated with other PCS machinery components (compressors and expanders), ultimately justifying the advantages of operating at higher storage pressures.

1. Introduction

Compressed air energy storage (CAES) and advanced adiabatic CAES (AA-CAES) are not assessed sufficiently from the economic perspective. The main difference between an AA-CAES and a conventional CAES plant centres on the thermal energy storage which is primarily achieved through using heat exchangers (HXs). It is widely acknowledged that AA-CAES can efficiently reduce cost of power generation in comparison to CAES plants [1–4].

HXs play a pivotal role in enhancing the efficiency and overall performance of most power generation plants. The available state-of-the-art literature in this area can be categorized into two parts: those focused on the thermal/thermodynamic performance of HXs [5–9] and those exploring trade-offs between cost and thermal performance to achieve an optimum design [1–4,10–17]. Nevertheless, a comprehensive evaluation of the impact of operating pressure on the overall cost of HX units has been conspicuously absent from the existing literature on CAES.

The following provides a concise overview of the most recent papers in both areas:

Khosravi et al. [5] explored a novel approach for small-scale CAES, proposing a double pipe heat exchanger with nanofluid to cool compressed air before storage. Their study involved nine different internal tube geometries, modelled using computational fluid dynamics to assess nanofluid and geometry effects on performance. Results showed a consistent pressure drop across finned tubes, and the analysis of cavern charging demonstrated temperature decline with increased secondary fluid mass flow. The proposed HX, exhibited up to a 22 % increase in convective heat transfer coefficient, emphasizing the potential of the finned tube and nanofluid combination for enhanced heat exchanger performance.

Kowalczyk [6] innovated a gas–gas system with two gas turbines, CAES and thermal energy storage (TES). The study introduces a detailed CAES-TES model, focusing on the main heat exchanger. Notable findings

* Corresponding author.
E-mail address: zahra.baniamerian@nottingham.ac.uk (Z. Baniamerian).

https://doi.org/10.1016/j.est.2024.111138
Received 30 November 2023; Received in revised form 21 February 2024; Accepted 28 February 2024
Available online 12 March 2024

Nomenclature

A	denotes the heat transfer area (m^2)
CA	Corrosion Allowance, (mm or in)
c_p	Specific heat capacity (J/kg. K)
d	Tube diameter (mm or in)
D	Shell diameter (mm or in)
E	Joint efficiency
F	Correction factor to indicate how the HX performs similarly to a counter current HX
F_t	Cost factor for design type
F_{pt}	Cost factor for pressure at the tube side
F_{ps}	Cost factor for design pressure at the shell side, and material of construction
F_m	Cost factor for material of construction
h	Convective heat transfer coefficient ($W/m^2.K$)
l	Overall tube length (m)
$\dot{m}$	Mass flow rate (kg/s)
M	Molecular weight of the gas (gr/mole)
N_t	Number of tubes
p	Pressure (bar)
Pr	Prandtl number
Q	Heat transfer within HXs (W)
Re	Reynolds number
R_{in}	Inside radius of tubes, (mm)
S_{all}	Maximum allowable stress (bar)
t	Thickness of tubes (mm or in)
T	Temperature (°C)
U	overall heat transfer coefficient (W/m^2K)
V	Velocity (m/s)

Greek symbols

μ	Dynamic viscosity (Pa.s)
ρ	Density (kg/m^3)

include a 34 % reduction in start-up heat loss. The study highlights improved environmental impact and heat exchanger performance for CAES.

Effects of HXs losses and pressure drops on the overall efficiency of the AA-CAES plants have been investigated by Yang et al. [7] for a single operating pressure. They found that the overall AA_CAES efficiency is influenced by the HX effectiveness with pressure loss exerting a more pronounced influence on the conversion of heat energy in thermal energy storage (TES) compared to internal energy of air.

Cardenas and Garvey [10] devised a heat storage unit with integrated HXs for CAES. This unit, charged directly by the system's pressurized air stream, eliminates the need for extra heat exchangers, streamlining the process. In a medium-scale CAES system case study, the integrated TES + HX unit, costing £38.5k, achieves a levelized cost of ~35 £/MWh and an overall roundtrip exergy efficiency of ~91.8 %. This design not only reduces the capital cost and improves efficiency but also simplifies the overall CAES system architecture.

Guo et al. [11] conducted a study aimed at developing thermodynamic and economic models for CAES systems. According to their findings, HXs contribute significantly to the cost, accounting for half of the expenditure on compressors and roughly two-thirds of the expander costs. However, their work does not explore the effect of storage pressure on these expenditures.

As mentioned previously, the current HX literature dominantly focuses on thermal, thermodynamic, and exergoeconomic aspects. However, a notable gap exists regarding the impact of operating pressure on both the cost and thermal performance of heat exchangers. Existing research often opts for a specific operating pressure without conducting a thorough evaluation of its influence on the overall cost of HX units. This literature gap underscores the necessity for studies specifically addressing the interplay between operating pressure, cost, and thermal performance in the context of AA-CAES.

When considering the presence of multiple AA-CAES plants with varying ultimate storage pressures, the overall plant typically incorporates several compression stages with different outlet pressures. As demonstrated in Part I, this operating pressure significantly impacts the cost of power conversion system (PCS) machinery. Part I specifically examined compressors and expanders, revealing that the cost per unit of power for compressors and expanders decreases as the pressure within the stages increases. In other words, it was established that compressors in the second compression stage, despite absorbing same power, have lower costs compared to those in the first stage, and this trend continues in subsequent stages. Conversely, in the case of expanders, as the pressure decreases within the stages, the first-stage expander exhibits the lowest cost, with costs rising in subsequent expansion stages. In the present study, a similar procedure is conducted for HXs to examine how the size, thermal performance, and cost of HXs in different compression stages vary with pressure. In this regards, the engineering rationale behind the relationship between operating pressure and HX design and cost is comprehensively assessed, providing valuable insights to the field of AA-CAES.

The novelty of this paper lies in two aspects: First, its comprehensive exploration of how pressure influences the size and cost of an HX designed for specific thermal performance goals. The study evaluates specific thermal performance in the application of AA-CAES across different operating pressures, revealing distinctions in the designed HXs. Despite their shared thermal objectives, these HXs exhibit variations influenced by diverse pressure conditions. Second, an innovative cost estimation method for heat exchangers, which is customized not only to consider the effects of intake pressure on the overall weight/size and consequently the costs of HXs but also to provide an effective cost estimation based solely on the thermal design of an HX.

2. Methodology

In Fig. 1, a schematic of a 4-stage compression/expansion AA-CAES system is shown. It employs similar HXs for intercooling and aftercooling during compression stages. The figure displays inlet and outlet temperatures for cold and hot streams.

As was shown in Part I, this study considers various storage pressures within the range of 10–350bar. The number of compression stages is calculated based on a compression ratio of 2.42 for each compression stage. This compression ratio ensures that the outlet air temperature from the compressors never exceeds 100 °C, enabling the utilization of non-pressurized water for sensible heat storage.

For instance, to achieve the maximum pressure of 350 bar in this study, 7 compression stages are needed, which results in the incorporation of 7 HXs. While the compressors absorb identical power, and compression ratios (likewise for expanders), the HXs are identical from a thermal design perspective.

The objective of the present work is to explore how the cost of similar heat exchangers, vary against operating pressure as proceeding through the compression/expansion stages.

3. Effects of pressure on size and performance of heat exchangers

The air emerging from each compression stage is cooled down to ambient temperature by a HX. This heat must then be transferred to the air before it enters each expander within the expansion stages. As the air

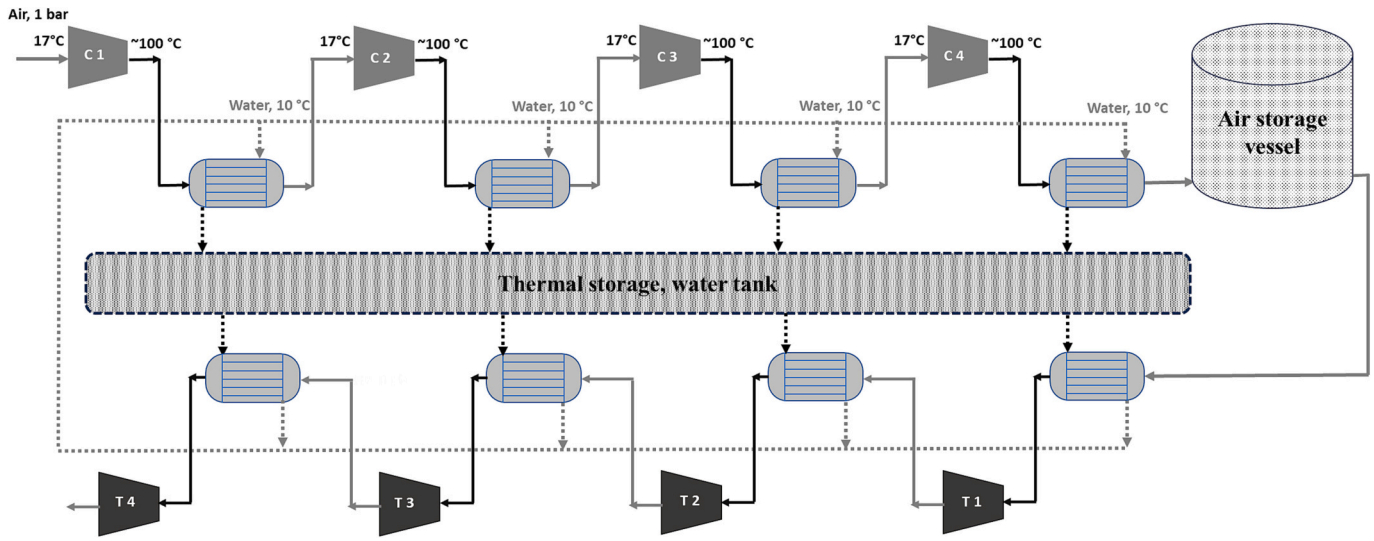

Fig. 1. Inlet and outlet temperature in a 4 stage-compression-expansion unit.

flows from one compression/expansion stage to the next, its pressure varies. Consequently, the air pressure entering each heat exchanger is not consistent. The consistent inlet and outlet air temperatures for all compressors/expanders indicate similar thermal design for the HXs. Nevertheless, differences in operating pressures may result in difference in HXs mechanical designs. This section investigates how intake pressure impacts the size, weight, and cost of the HXs used in AA-CAES plant.

To enable a simple comparison, two heat exchangers are considered separately. The heat exchanger, HX_A, as shown in Fig. 2, intakes air with pressure $p_{in,\ A}$ and temperature T_{in} and the second heat exchanger, HX_B has suction pressure of $p_{in,B}$ ($\frac{p_{in,B}}{p_{in,A}} : \Pi > 1$) and similar inlet temperature T_{in}. The pressure at the water side is identical for both HXs.

Assumptions during this analysis are:

- Both HXs are assumed to be shell and tube.
- Hot flow and cold flow streams in both HXs are similar in temperature and mass flow rates.
- Water is chosen as the cooling fluid for both HXs.
- Thermophysical properties of the fluids are assumed constant.

3.1. Type of HX

As shown in Fig. 2, the mean temperature within the hot side is $\frac{100+17}{2} = 58.5^{\circ}C$, and can be further shown that the mean temperature within the cold side of both heat exchangers would be $<50\ ^{\circ}C$. Since the difference between hot-side and cold-side mean temperatures is $<50\ ^{\circ}C$, the fixed tube sheet at both heads would be a good choice [18]. BEM/BEU type shell and tube heat exchangers are selected in this study.

3.2. Flow arrangement

High pressure flow should be routed through the tubes; hence, air flows within the tubes and water flows through the shell. Square 90° pattern is assumed for the tubes' layouts in both HXs to facilitate cleaning and maintenance in the shell side.

3.3. Diameter and thickness of tubes and shell

Compact HX units are achieved through the utilization of small-diameter, densely arranged tubes, which are advantageous for heat transfer efficiency. However, in the present case where water flows within the shell, this arrangement presents challenges in terms of cleaning, necessitating adequate space for de-fouling procedures. The use of large-diameter, widely spaced tubes mitigates cleaning issues but sacrifices efficient heat transfer due to reduced compactness. To obtain the lowest cost HX for a given surface area, tubes should be selected as small in diameter and as long as possible, consistent with the space and handling facilities. Tube branches of 6 m long (which yields to a 3 m long shell) are considered in this study. In heat transfer applications, the typical outside tube diameter ranges from 3/4 to 2 in., with 3/4 and 1-in. diameters being the most prevalent.

3.4. Effects of pressure on the designs of shell and tubes

Tube and shell thicknesses are evaluated against internal and external pressures. For this purpose, the thicknesses of tubes across the entire range of considered pressures are computed using "Lamé" equation and subsequently assessed for their commercial availability.

The minimum thickness, t for a tube with an inside radius R_{in}, required to withstand the internal air pressure, p_{in} is determined as follow:

$$t = \frac{p_{in}R_{in}}{S_{all}E - 0.6p_{in}} + CA \tag{1}$$

The joint efficiency, E is considered 1 for the seamless pipes, 0.6 for the furnace butt-welded pipes, and 0.85 for electric-resistance welded pipes. CA is the corrosion allowance which is considered 1 mm for the

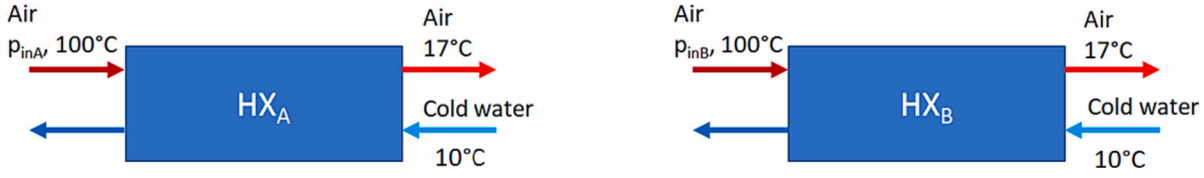

Fig. 2. Schematic of the two compared heat exchangers.

case of compressed air in tubes [18]. The selected material for tubes in heat exchanger applications is Carbon Steel SA 333 grade 1 with maximum allowable stress of 1080 bar.

To determine suitable tube sizes for the current HXs, diameters of 3/4 in., 1 in., 1 ½ inches, and 2 in.—the most popular diameters—were evaluated and compared. For each tube diameter, the necessary tube thickness was calculated for every pressure within the specified pressure range using Eq. (1). The resulting thicknesses were then examined for commercial availability in BWG and IPS tube gauges.

Among the BWG tube gauges, none met the specified thickness requirement across the considered pressure range. However, certain IPS tube gauges were found to be suitable for safe utilization across the range of pressures examined in this study. The results of the tube selections are presented in Table 1. As a rough comparison, a 1-in. tube capable of withstanding 250 bar pressure weighs 4.26 kg/m. In normal atmospheric operating pressure, due to the need for lower thicknesses, the aforementioned 1-in. tube weighs approximately half, 2.1 kg/m.

Regarding the shell thickness, when the high-pressure fluid is non-explosive, as in the current study, the shell can be designed to accommodate normal operation at 3.5 bar. Additionally, it can be equipped with a pressure safety valve to manage situations such as tube rupture or leakage.

The necessary shell diameter, required to house the designated number of tubes in a certain layout, is found from [19]. Consequently, for each considered pressure level, the shell diameter and thickness collectively determine the weight of the shell.

At first glance, Table 1 shows that increase in the operating pressure would correspondingly elevate the weight of the heat exchanger and subsequently the associated cost. However, this is not a complete assessment, as the operating pressure also impacts the overall heat transfer process and, consequently, the required heat transfer area. This matter will be explored in the following section.

3.4.1. Thermal design of HXs

The total heat transfer by the hot flow and the cold flow, Q within a HX is calculated by:

$$Q = \left(\dot{m}c_p\right)_{water}\Delta T_{water} = \left(\dot{m}c_p\right)_{air}\Delta T_{air} \tag{2}$$

Table 1
Suitable IPS tubes that satisfiy the required thickness criterion.

P (bar)	Tube outside diameter (in)	Required thickness calculated by Eq. (1) (In)	Appropriate IPS tube	Weight per length of tube	
				Lb/ft	Kg/m
250	3/4	0.23	XX	2.44	3.66
	1	0.26	XX	2.84	4.26
	2	0.39	XX	9.03	13.55
200.93	3/4	0.21	160	1.94	2.91
	1	0.23	160	2.17	3.255
	2	0.34	160	7.45	11.18
83.03	3/4	0.16	80/XS/80S	1.47	2.21
	1	0.17	80/XS/80S	1.68	2.52
	2	0.21	80/XS/80S	5.02	7.53
34.31	3/4	0.14	80/XS/80S	1.47	2.21
	1	0.14	80/XS/80S	1.68	2.52
	2	0.16	80/XS/80S	5.02	7.53
14.18	3/4	0.13	80/XS/80S	1.47	2.21
	1	0.13	40/STD/40S	1.4	2.1
	2	0.14	40/STD/40S	3.65	5.48
5.86	3/4	0.13	80/XS/80S	1.47	2.21
	1	0.13	40/STD/40S	1.4	2.1
	2	0.13	40/STD/40S	3.65	5.48
2.42	3/4	0.13	80/XS/80S	1.47	2.21
	1	0.13	40/STD/40S	1.4	2.1
	2	0.13	40/STD/40S	3.65	5.48
1	3/4	0.12	80/XS/80S	1.47	2.21
	1	0.12	40/STD/40S	1.4	2.1
	2	0.13	40/STD/40S	3.65	5.48

$$Q = UAF\Delta T_{LMTD} \tag{3}$$

$$\Delta T_{LMTD} = \frac{\Delta T_{one\ end} - \Delta T_{the\ other\ end}}{ln\frac{\Delta T_{one\ end}}{\Delta T_{the\ other\ end}}} \tag{4}$$

$$A = N_t(\pi dl) \tag{5}$$

The hydrodynamic method based on considering the maximum possible flow velocities for the fluids flows within the tubes is applied for designing the present HXs. The maximum velocity for the gases, $V_{max,gas}$(m/s) flowing within tubes depends on the operating pressure [20]:

$$V_{max,gas} = \frac{144}{(pM)^{0.5}} \tag{6}$$

The maximum velocities are based on avoiding vibration as well as prevention of tube wall erosion and are material specific. The above equation is proposed for carbon steel tubes and in cases of having different materials a correction factor should be considered [20].

3.4.2. Effects of pressure on overall HTC of HXs

The overall HTC within the HX, can be simply calculated by the following equation:

$$U_o = \frac{1}{\frac{A_o}{A_i}\frac{1}{h_i} + A_oR_w + \frac{1}{h_o}} \tag{7}$$

where A_o and A_i (m^2) are outside and inside areas of the tubes respectively. h_o, and h_i (W/m^2K) respectively represent convective HTC within the shell side and the tube side. R_w ($m^2.K/W$) is the wall thermal resistance in HXs. The latter is the same for both considered HXs due to use of similar material and geometry.

Convective HTCs in tubes and shell can be calculated from the Nusselt number at each side for which the following equations are widely applied [19]:

$$Nu_{tubes} = 0.021Re_d^{0.8}Pr^{0.4} \tag{8}$$

$$Nu_{Shell} = 0.2Re_D^{0.6}Pr^{0.4} \tag{9}$$

Re denotes the Reynolds number and *Pr* denotes the Prandtl number.

$$Re_W = \frac{4\dot{m}_W}{\pi D_{sh}\mu_W} \tag{10}$$

$$Re_{air} = \frac{\rho_{air}V_{air}d}{\mu_{air}} \tag{11}$$

where, index *W* represents water. Now recall the two HXs under consideration; Namely that the operating pressure within the tube side of HX_B is Π times that of HX_A. Consequently, the air density in the HX_B is Π times greater than HX_A. With reference to Eq. (5), the maximum air velocity diminishes with pressure by a factor $\frac{1}{\sqrt{\Pi}}$. As a result, the air Reynolds number in HX_B, $Re_{air}|_B$ becomes $\sqrt{\Pi}$ times the air Reynolds number in HX_A, $Re_{air}|_A$. According to the observed increase in *Re*, the HTC in HX_B might be $\Pi^{0.4}$ times the HTC in HX_A.

$$h_{air}|_B = \Pi^{0.4}h_{air}|_A \tag{12}$$

By performing an order of magnitude calculations, it can be simply shown that:

$$U \sim h_{air} \tag{13}$$

Having Eq. (11) together with Eq. (12), in consideration, the following can be argued:

$$U|_B \cong \Pi^{0.4}U|_A \tag{14}$$

With Eqs. (3) and (5), in addition to Eq. (14), and considering that

the inlet and outlet temperatures of both flows are set similarly for HX_B and HX_A, and both heat exchangers have similar tube diameters, one can conclude that:

$$\frac{(N_t \times l)|_A}{(N_t \times l)|_B} = \frac{U|_B}{U|_A} \cong \Pi^{0.4} \tag{15}$$

While order-of-magnitude analysis can provide an estimation of the change in overall heat transfer and the dimensions of HX_B compared to HX_A, it may not fully capture the practical implications. To address the impact of pressure on overall heat transfer and consequently the size of HX, the heat transfer of the shell side (water flow) also needs to be evaluated. Given that the number of tubes in the hydrodynamic-based design procedure is directly calculated based on the maximum tube velocity, the shell diameter required to accommodate these tubes becomes a function of the calculated maximum tube velocity. Consequently, the Reynolds number within the shell is also affected.

To comprehensively investigate the effect of pressure on HX size and cost, ten different HXs are individually designed. The air pressures for these ten HXs are set at 1, 2.42, 5.86, 14.17, 34.3, 83, 200, 250, 300, and 350 bar respectively. The following assumptions have been taken into consideration:

- Air mass flow rate is assumed constant for all HXs.
- Air velocities within the tubes are set based on the maximum allowable velocity, Eq. (5).
- Double pass tubes are considered (U-bundle).
- The HXs are assumed to be 3 m long with 6 m long tubes.

Based on the data obtained from designing the mentioned ten HXs, the variation of overall HTC against pressure is depicted in Table 2. All data presented in this table, excluding the maximum air velocity, has been normalized with respect to the corresponding data for the HX operating at atmospheric pressure, rendering them as relative values. For instance, the relative air Reynolds number signifies the air Reynolds number at a given pressure relative to the Reynolds number at atmospheric pressure. Notably, it becomes evident that the overall HTC exhibits a proportionality of approximately $p^{0.375}$:

$$U \propto p^{0.375} \tag{14}$$

In other words, the HX_B with operating pressure of Π times that of HX_A would experience overall HTC of $\Pi^{0.375}$ times that of HX_A.

$$\frac{U|_{HX_B}}{U|_{HX_A}} = \Pi^{0.375} \tag{15}$$

This means that the required heat transfer area will shrink by increasing the operating pressure by the factor $\Pi^{0.375}$ (Fig. 3).

Thus far, two distinct effects resulting from an increase in operating pressure on heat exchangers have been examined. The initial effect, discussed in the preceding section, disclosed an increase in the required thickness of tubes and shell, signifying a rise in costs. The second effect, more recently identified, involves a decrease in the thermal heat transfer area (including the number of tubes and subsequently the shell diameter), leading to cost reduction. To address both of these effects, the optimal approach is to establish a trendline depicting the relationship between cost and pressure across all designed HXs.

3.4.3. Effects of pressure on overall cost of HXs

Two distinct methods are employed in this study to approximate the cost of heat exchangers. The initial method, similar to what was accomplished for compressors and expanders, in Part I, utilizes the "Rule of Thumb" to estimate the cost of the heat exchanger based on its dimensions. The second method approximates the cost of the heat exchanger by considering its weight, assuming a manufacturing price per unit weight. The "Rule-of-Thumb" to approximate the cost of shell and tube HXs is in the following form [21]:

$$Cost_2 = Cost_{ref}\left(\frac{Heat\ transfer\ area_2}{Heat\ transfer\ area_{ref}}\right)^n \tag{16}$$

where n is suggested to be 0.71 for the shell and tube HXs with heat transfer areas in the range of 20–2000 m^2.

With reference to what has been already obtained, the cost of HX_B would be:

$$Cost\ of\ HX_B = Cost\ of\ HX_A\left(\frac{1}{\Pi^{0.375}}\right)^n \tag{17}$$

In the case of the heat exchangers within the compression unit examined in this study, the "Rule of Thumb" indicates that the variation of cost against the operating pressure follows a proportionality of approximately $p^{(-0.266)}$, as detailed in Table 3.

It is worth noting that the "Rule of Thumb" is only valid up to the pressures around 200 bar. Beyond this point, the increase in weight due to higher thickness requirements outweighs the reduction in thermal area, making this rule impractical.

The second approach for estimating the cost of HXs is to derive their cost as a function of their weight. This has been accomplished for the ten designed HXs. By considering the overall weight of each HX and taking material and manufacturing expenses into consideration, it becomes possible to approximate HX cost against operating pressure.

To accomplish weight approximation based on the second approach, a trendline linking the area to weight for heat exchangers operating at varying pressures is established (Fig. 4). This trendline aids in making effective comparisons. Fig. 5 shows the variation of relative weight/area ratio which accounts for the ratio of weight per required thermal area for the various designed heat exchangers at different operating pressures. Guided by this trendline, when conducting the thermal design for a heat exchanger to determine the required heat transfer area, the HX weight can be calculated and subsequently compared across different operating pressures.

The data obtained, based on the second approach (analytical design), indicates that the cost of a HX experiences a decrease corresponding to

Table 2
Variation of various heat transfer parameters in HXs with pressure.

P, bar	Max air velocity (m/s)	Relative air Re	Relative HTC of air W/m2	Relative water *Re*	Relative HTC of water W/m2	Relative overall HTC (W/m2K)	Density of air (kg/m3)	Relative overall tubes length	Relative N_t	Relative shell diameter
1	26	1	1	1	1	1	1.29	1	1	1
2.42	17	1.45	1.35	1.1	1.23	1.31	2.91	1.09	0.7	0.84
5.86	11	2.26	1.91	1.24	1.57	1.8	7.04	1.23	0.45	0.73
14.17	7	3.5	2.72	1.52	2.20	2.54	17	1.36	0.29	0.57
34. 3	4	5.45	3.88	1.87	3.08	3.58	41	1.48	0.18	0.46
83	2.5	8.69	5.63	2.18	4.10	5.65	102	1.68	0.12	0.41
200	1.8	13.7	8.1	2.39	5.05	6.83	250	1.92	0.08	0.32
250	1.7	15.29	8.84	2.66	5.89	7.65	311	1.94	0.07	0.30
300	1.5	16.75	9.51	2.76	6.03	7.93	374	2.03	0.06	0.30
350	1.4	18.09	10.12	2.99	6.95	8.87	436	1.92	0.06	0.27

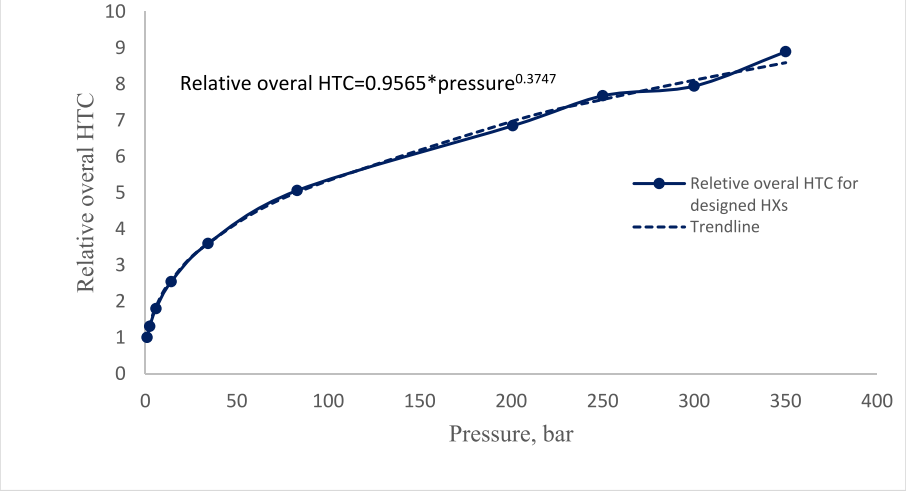

Fig. 3. Variation of relative overall HTC in various operating pressures.

Table 3
Variation of cost of HX against operating pressure based on the "Rule of Thumb".

Operating pressure (bar)	Relative cost of HX
1	1
2.42	$=\left(\frac{1}{2.42^{0.375}}\right)^{0.71}=0.79$
5.86	$=\left(\frac{1}{5.86^{0.375}}\right)^{0.71}=0.628$
14.17	$=\left(\frac{1}{14.17^{0.375}}\right)^{0.71}=0.498$
34.3	$=\left(\frac{1}{34.3^{0.375}}\right)^{0.71}=0.395$
83	$=\left(\frac{1}{80^{0.375}}\right)^{0.71}=0.314$
200	$=\left(\frac{1}{200^{0.375}}\right)^{0.71}=0.244$

the operating pressure raised to the power of 0.28 just up to pressure 200 bar and starts to increase afterward.

In other words, the trend shown in Table 3, based the "Rule of Thumb" (first approach) satisfies the analytical design with a good accuracy up to the pressure 200 bar as illustrated in Fig. 5. Nevertheless, as the operating pressure continues to rise, the rate of weight increase surpasses the rate of area reduction. Consequently, heat exchangers operating beyond 200 bar experience the overall weight increase and as a result cost increase. Fig. 5 demonstrates the variation of relative cost approximation based on the two mentioned approaches.

Fig. 6 shows the weight variation for a single HX against operating pressure and as a result, the estimated cost, which is based on the weight of the HX, reaches a turning point at 150 bar and begins to incline upwards.

This means that in a multi-stage compression train with multiple similar thermally performing heat exchangers, the first HX would be the most expensive one. As we proceed through the compression stages, the HXs, despite providing similar thermal performance, shrink and become more cost-effective. However, for higher pressures, the cost of the HX experiences an increase. A similar trend occurs in opposite direction for the expansion unit.

Fig. 7 illustrates the weights of the shell and tubes for various considered tube diameters within the specified pressure range. According to this figure, the optimal choice appears to be the 1-in.

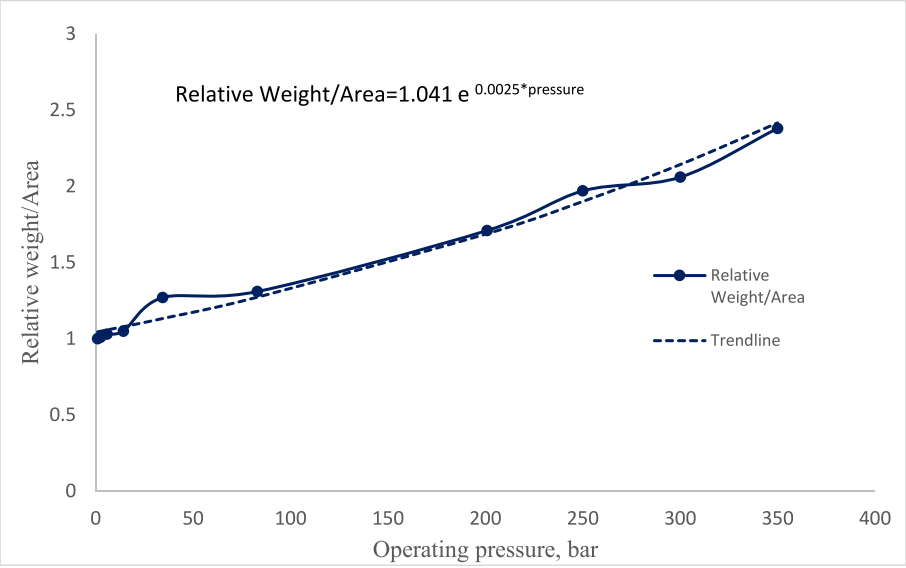

Fig. 4. A trendline fitted over the data obtained from the ten designed HXs at various operating pressures to link the weight of HX to its heat transfer area.

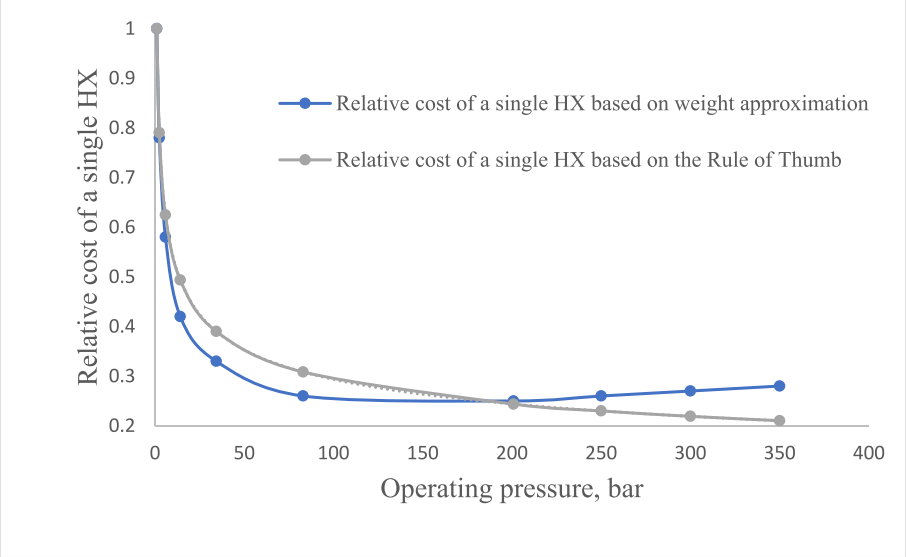

Fig. 5. Variation of relative cost of HXs against pressure based on the weight approximation and the "Rule of Thumb".

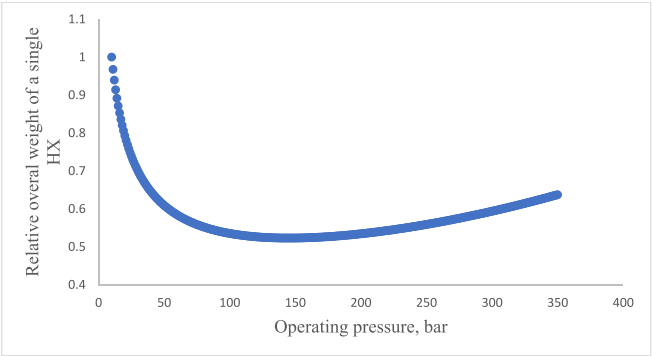

Fig. 6. Variation of relative overall weight of a single HX against pressure.

diameter tubes, resulting in the lightest possible heat exchanger.

4. Verification of the model

To validate the methods used for cost estimation, considering the effects of pressure, the Erwin's theory has been employed. According to Erwin's theory, the base cost of shell and tube HXs is calculated as follows:

$$Total\ base\ cost = base\ cost \times \left(F_t + F_m + F_{pt} + F_{ps}\right) \times escalation\ index$$

The base costs are calculated based on the surface area of floating-head shell and tube HXs using carbon steel for both the shell and tubes (Fig. 8). Cost factors F_t, F_{pt}, F_{ps}, F_m account for design type, design pressure at the tube side, design pressure at the shell side, and material of construction, respectively. These factors can be obtained from the tables provided in the reference.

The escalation index represents the yearly increase of the specific equipment item. However, in our comparison, as all costs are calculated relative to the heat exchanger at ambient operating pressure, this index would be the same for both HXs and excluded.

Erwin's theory considers only pressures of 100, 1000, and 2000 psi for the tube side. Nevertheless, interpolation is permitted within the specified pressure ranges.

Table 4 provides detailed calculations of costs for the various considered pressures according to Erwin's theory.

A comparison of the calculated relative costs for the heat exchanger, based on the Rule of Thumb, Erwin's theory, and the present study, is presented in Table 5. As mentioned earlier, the Rule of Thumb does not account for the mass increment due to thickness increase for pressures exceeding 200 bar. Erwin's theory, on the other hand, considers pressures up to approximately 140 bar. However, for the pressures available in the present study, the results exhibit a high level of consistency with both theories.

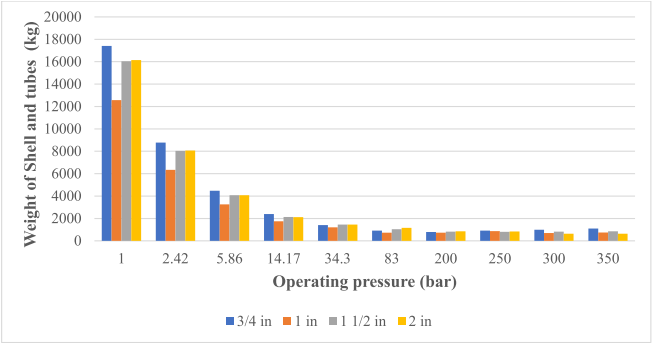

Fig. 7. Variation of relative overall weight of a single HX against pressure.

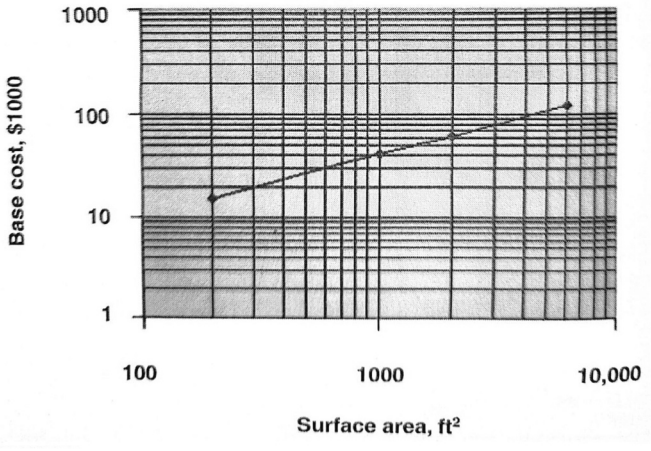

Fig. 8. Shell and tube HXs base cost [22].

Table 4
detailed calculations of costs for the various considered pressures according to Erwin's theory.

P (bar)	A (m^2)	A (ft^2)	Base cost, $1000	F_t	F_m	F_{pt}	F_{ps}	Sum of cost factors	Total cost ($1000)	Relative Total cost
1	562.58	6055.574	140	0.84	1.85	0.03	0.03	2.75	385	1
2.42	429.87	4627.132	100	0.84	1.75	0.03	0.03	2.65	265	0.69
5.86	312.97	3368.772	75	0.85	1.7	0.05	0.03	2.63	197.250	0.51
14.17	221.33	2382.371	70	0.85	1.69	0.051	0.03	2.621	183.470	0.48
34.30	156.43	1683.764	59	0.85	1.67	0.055	0.03	2.605	153.695	0.4
83.00	111.19	1196.875	45	0.85	1.66	0.07	0.03	2.61	117.450	0.31

Table 5
Relative costs; comparison from different models.

Operating pressure (bar)	Relative cost of HX		
	The rule of thumb	Erwin's theory	Present study
1	1	1	1
2.42	0.79	0.69	0.78
5.86	0.63	0.51	0.58
14.17	0.5	0.48	0.42
34.3	0.4	0.4	0.33
83	0.314	0.31	0.26
200	0.244	Not applicable	0.25
250	0.23	Not applicable	0.26
300	0.22	Not applicable	0.27
350	0.21	Not applicable	0.28

5. Results and discussion

As illustrated in Fig. 1, the inlet and outlet temperatures are consistent across all HXs, resulting in similar thermal performance. Fig. 9 demonstrates the variation in the cost of incorporated HXs in AA-CAES plants at various storage pressures. The analyses conducted indicate that the HXs gradually decrease in size as they progress through the compression stages. However, for the HXs at pressures above around 200 bar, due to enhanced weight increase, the cost per kW tends to slightly increase with pressure. Based on the performed assessment, the first-stage HX in the compression units is the most expensive one, and as we proceed within the stages, due to the increase in pressure, the costs of the HXs decline. There's a noticeable jump in the cost of HXs for storage pressures ranging from 85 to 200 bar. Beyond the 200-bar threshold, the cost of HXs surpasses that of compressors/expanders. This has been discussed in detail in Part I.

The cost contribution of each machine at various storage pressures is illustrated in Fig. 6, which is located in Part I of the paper. This figure illustrates that the cost contribution of compressors and expanders decreases as storage pressure increases, whereas for the HXs, the cost contribution increases with rising storage pressure. As an illustration, compressors make up 43 % of machinery cost at 30 bar and 31 % at 350 bar. Expander costs range from 47 % to 34 % between 30 and 350 bar; However, HX costs increase from 10 % at 30 bar to 35 % at 350 bar.

6. Conclusion

This study thoroughly examined the impact of pressure on the size and cost of a HX designed to achieve specific thermal performance goals in the application of AA-CAES. In this context, a consistent thermal performance was assessed under various operating pressures to observe the differences in the designed HXs, all aiming to meet the same thermal objectives but influenced by different pressure conditions. The analyses focused on integrating the effects of operating pressure on the size of key components in HXs, providing a comprehensive view of their impact on design and cost.

An innovative cost estimation method for the heat exchangers was customized to consider the effects of intake pressure on the overall weight/size and consequently the costs of HXs as well. The following are

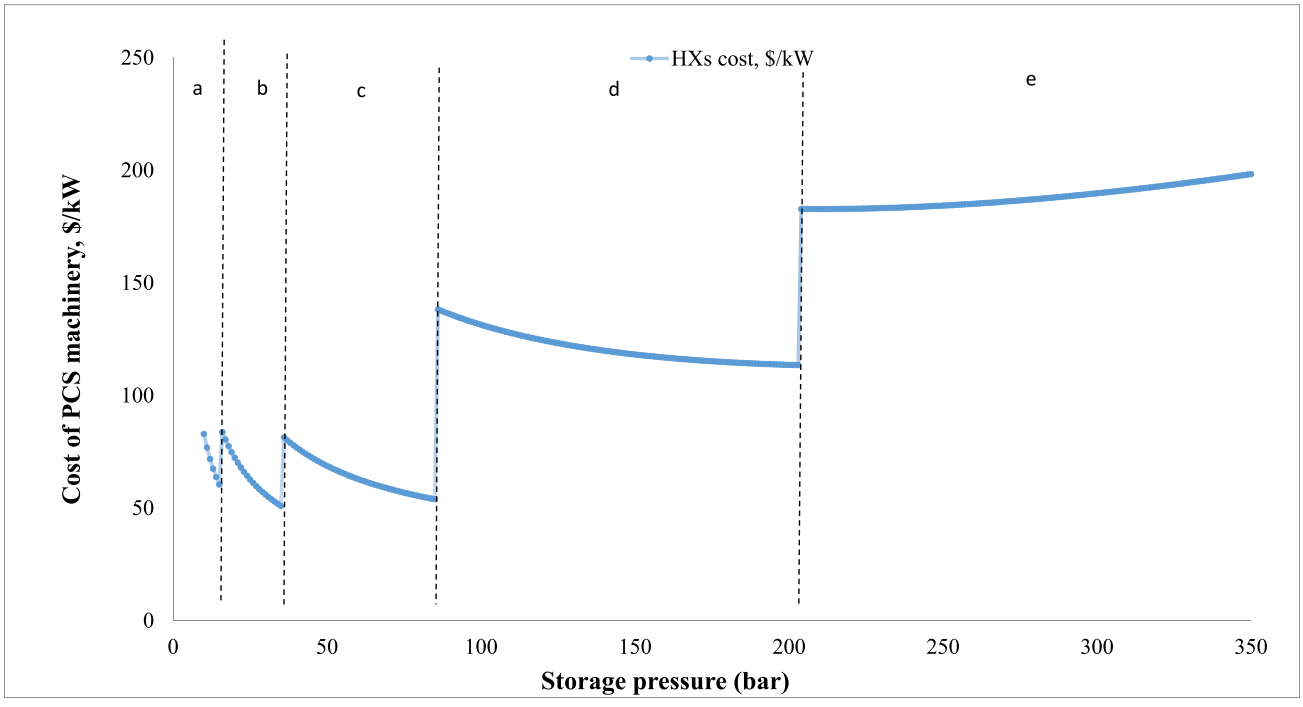

Fig. 9. Cost of HXs vs storage pressure $/kW.

some concluding remarks based on the performed analysis:

- The operating pressure of a HX impacts two crucial cost-related factors: the heat transfer area and required tube thicknesses. Higher operating pressures are associated with the smaller heat transfer area and lowers costs, but increasing pressure raises tube thickness requirements, leading to increased costs. Below approximately 200 bar, the former effect prevails over the latter, leading to cost reductions with rising pressure. Conversely, at higher pressures, the latter effect outweighs the former, resulting in cost increases with increasing pressure.
- The relative overall HTC of a HX is a reliable indicator of how pressure influences the overall HTC compared to operation at ambient pressure. This value increases with pressure, following a power of 0.375. For instance, at 100, 200, 300, and 350 bar, the overall HTC would be almost 5.5, 7, 8, and 9 times the HTC at ambient pressure, respectively.
- The overall relative weight (ORW) of a HX provides a reliable estimate of how pressure affects the weight of the HX compared to one operating at ambient pressure. The ORW decreases from 1 to 0.53 as the pressure increases from ambient to 200 bar and subsequently rises to 0.64 for a pressure of 350 bar.
- The “Rule of Thumb” for approximation of HXs' cost satisfies the analytical design with a good accuracy up to the pressure 200 bar. Nevertheless, as the operating pressure continues to rise, the rate of weight increase surpasses the rate of area reduction. Consequently, heat exchangers operating beyond 200 bar experience an overall weight increase and as a result cost increase.
- As the number of compression stages is increased to attain higher storage pressures, there is a noteworthy variation in the cost contribution of HXs. Specifically, the contribution of HX costs within the PCS machinery escalates from 10 % at a storage pressure of 30 bar to approximately 35 % at a storage pressure of 350 bar. This cost increase is accompanied by a substantial reduction in the expenses associated with other PCS machinery components (compressors and expanders), ultimately justifying the advantages of operating at higher storage pressures.

In the future, there are several potential research directions stemming from the findings of this study. Subsequent studies could investigate strategies to optimize storage pressure for cost-effectiveness, considering dynamic operational costs and ensuring the long-term economic sustainability of AA-CAES plants. The inclusion of thermal storage costs in the thermal section further enhances the value of advancing this research. Additionally, the study's conceptual engineering approach has paved the way for refining cost correlations in HXs, with consideration for the influence of operating pressure. Future research efforts could expand upon these enhancements, refining cost estimation models specifically tailored for HXs not only in the context of AA-CAES but also in any application of HXs.

CRediT authorship contribution statement

Zahra Baniamerian: Writing – original draft, Visualization, Validation, Software, Resources, Methodology, Investigation, Formal analysis, Data curation, Conceptualization. **Seamus Garvey:** Writing – review & editing, Supervision, Project administration, Funding acquisition, Conceptualization. **James Rouse:** Writing – review & editing, Methodology. **Bruno Cárdenas:** Writing – review & editing, Methodology. **Daniel L. Pottie:** Writing – review & editing, Methodology. **Edward R. Barbour:** Writing – review & editing, Funding acquisition. **Audrius Bagdanavicius:** Writing – review & editing, Funding acquisition.

Declaration of competing interest

The authors declare that they have no known competing financial interests or personal relationships that could have appeared to influence the work reported in this paper.

Data availability

Data will be made available on request.

Acknowledgement

The authors would like to thank the United Kingdom's Engineering and Physical Sciences Research Council (EPSRC) for supporting this work through the following research grant: ‘Sustainable, Affordable and Viable Compressed Air Energy Storage’ (EP/W027569/1). The authors would also like to express their gratitude to the reviewers who contributed to improving the quality of this paper.

References

[1] Y. Li, S. Miao, S. Zhang, B. Yin, X. Luo, M. Dooner, J. Wang, A reserve capacity model of AA-CAES for power system optimal joint energy and reserve scheduling, Int. J. Electr. Power Energy Syst. 104 (2019) 279–290.
[2] M. Zarnoush, P.P. Golaki, M. Soltani, E. Yamini, F. Esmaeilion, J. Nathwani, Comparative evaluation of advanced adiabatic compressed gas energy storage systems, J. Energy Storage 73 (2023) 108831. Part A.
[3] D. Wu, W. Wei, J. Bai, S. Mei, Optimal bidding strategies of advanced adiabatic compressed air energy storage based energy hub in electricity and heating markets, J. of Energy Storage 62 (2023) 106770.
[4] E.H. Güleryüz, D.N. Özen, Advanced exergy and exergo-economic analyses of an advanced adiabatic compressed air energy storage system, J. Energy Storage 55, Part D (2022) 105845.
[5] A. Khosravi, H. Campos, M. Malekan, R.O. Nunes, M.E.H. Assad, L. Machado, G. Pabon, Performance improvement of a double pipe heat exchanger proposed in a small-scale CAES system: an innovative design, Appl. Therm. Eng. 162 (5 November 2019) 114315.
[6] T. Kowalczyk, Comparative analysis of hybrid energy storage based on a gas–gas system and a conventional compressed air energy storage based on a recuperated gas turbine round trip efficiency, exergy losses, and heat exchanges start-up losses, Energy Convers. Manag. 258 (15 April 2022) 115467.
[7] K. Yang, Y. Zhang, X. Li, J. Xu, Theoretical evaluation on the impact of heat exchanger in advanced adiabatic compressed air energy storage system, Energ. Conver. Manage. 86 (2014) 1031–1044.
[8] A.M. Abdelmoety, M.W. Muhieldeen, W.Y Tey, W. Yin, N.E. Beit, Numerical investigations on optimised shell designs of a U-tube heat exchanger, Therm. Sci. Eng. Process. 47 (2024) 102327.
[9] P. Prajapati, B.D. Raja, H. Savaliya, V. Patel, H. Jouhara, Thermodynamic evaluation of shell and tube heat exchanger through advanced exergy analysis, Energy 292 (2024) 130421.
[10] B. Cárdenas, Seamus Garvey, A directly charged thermal store for compressed air energy storage systems, J. Energy Storage 71 (1 November 2023) 108183.
[11] H. Guo, Y. Xu, Y. Zhu, X. Zhang, Z. Yin, H. Chen, Coupling properties of thermodynamics and economics of underwater compressed air energy storage systems with flexible heat exchanger model, Journal of Energy Storage 43 (2021) 103198.
[12] D. Fu, T. Nguyen, Y. Lai, L. Lin, Z. Dong, M. Lyu, Improved pinch-based method to calculate the capital cost target of heat exchanger network via evolving the spaghetti structure towards low-cost matching, J. Clean. Prod. 343 (1 April 2022) 131022.
[13] T.A. Patel, A. Kumar, V.K. Patel, Efficiency and cost optimization of offset plate-fin heat exchanger, materials today: proceedings, volume 77, Part 1 (2023) 142–147.
[14] A.J. Furlong, M.J. Pegg, Low-cost heat exchanger benches for remote operation, Educ. Chem. Eng. 44 (July 2023) 14–20.
[15] Z. Xia, S. Qin, Z. Tao, G. Jia, C. Cheng, L. Jin, Multi-factor optimization of thermo-economic performance of coaxial borehole heat exchanger geothermal system based on levelized cost of energy analysis, Renew. Energy 219 (Part 2) (December 2023) 119513.
[16] S. Sadeghi, S. Ghandehariun, M.A. Rosen, Waste heat recovery potential in the thermochemical copper–chlorine cycle for hydrogen production: development of an efficient and cost-effective heat exchanger network, Energy 282 (1 November 2023) 128357.
[17] H. Lin, F. Aldawi, S.A. Reda, Z.R. Abdulghani, S. Asaadi, H.S. Dizaji, Economic cost and thermal efficiency analysis of porous-minichannel heat exchanger for thermoelectric generator, Appl. Therm. Eng. 213 (August 2022) 118653.
[18] TEMA (Ed.), TEMA Handbook, 10th ed., TEMA Publishers, 2019.
[19] S. Kakac, Heat Exchangers: Selection, Rating, and Thermal Design, CRC Press, 2002.

[20] Robert W. Serth, Thomas G, in: Lestina, PROCESS HEAT TRANSFER PRINCIPLES, APPLICATIONS AND RULES OF THUMB, Second edition, Elsevier publishing, 2014.
[21] Donald R. Woods, Rules of Thumb in Engineering Practice, First edition, WILEY-VCH Verlag GmbH &Co. KGaA, 2007.
[22] Douglas L. Industrial Chemical Process Design, McGraw-Hill.